



## UvA-DARE (Digital Academic Repository)

### Controlling droplet deposition with surfactants

Hoffman, H.; Sijs, R.; De Goede, T.; Bonn, D.

**DOI**

[10.1103/PhysRevFluids.6.033601](https://doi.org/10.1103/PhysRevFluids.6.033601)

**Publication date**

2021

**Document Version**

Final published version

**Published in**

Physical Review Fluids

[Link to publication](#)

**Citation for published version (APA):**

Hoffman, H., Sijs, R., De Goede, T., & Bonn, D. (2021). Controlling droplet deposition with surfactants. *Physical Review Fluids*, 6(3), [033601].  
<https://doi.org/10.1103/PhysRevFluids.6.033601>




**General rights**

It is not permitted to download or to forward/distribute the text or part of it without the consent of the author(s) and/or copyright holder(s), other than for strictly personal, individual use, unless the work is under an open content license (like Creative Commons).

**Disclaimer/Complaints regulations**

If you believe that digital publication of certain material infringes any of your rights or (privacy) interests, please let the Library know, stating your reasons. In case of a legitimate complaint, the Library will make the material inaccessible and/or remove it from the website. Please Ask the Library: <https://uba.uva.nl/en/contact>, or a letter to: Library of the University of Amsterdam, Secretariat, Singel 425, 1012 WP Amsterdam, The Netherlands. You will be contacted as soon as possible.

## Controlling droplet deposition with surfactants

Hanne Hoffman , Rick Sijs , Thijs de Goede, and Daniel Bonn <sup>\*</sup>*Van der Waals-Zeeman Institute, University of Amsterdam Science Park 904, Amsterdam, Netherlands*

(Received 26 October 2020; accepted 16 February 2021; published 15 March 2021)

Droplets impacting on a surface are key to a wide range of applications such as spray deposition and inkjet printing. Yet, a full understanding of how they spread and retract is still lacking. Surfactants are often added to improve spreading and coverage of aqueous solutions, resulting in variations of the surface tension at timescales beyond the reach of conventional dynamic surface tension measurement methods. Here we study the impact dynamics of aqueous surfactant solutions on hydrophobic surfaces at millisecond timescales. We find that the spreading and retraction of droplets cannot be adequately described by the equilibrium surface tension. We infer the dynamic surface tension in the first milliseconds after impact from the spreading dynamics of droplets. “Slow” surfactants that take a lot of time to reach newly created droplet surface, only slightly decrease or even increase the surface tension, while “fast” surfactants, on the other hand, allow efficient wetting of aqueous solutions on hydrophobic surfaces. Our findings allow us to tailor surfactants for efficient drop deposition or spray application.

DOI: [10.1103/PhysRevFluids.6.033601](https://doi.org/10.1103/PhysRevFluids.6.033601)

### I. INTRODUCTION

The dynamics of droplets of complex fluids impacting on surfaces is of paramount importance for many applications. For example, in pesticide spraying, it is not unusual that over 50% of applied pesticide spray misses its target due to effects such as bounce-off and drift, ending up as environmental pollution [1]. For inkjet printing, the droplets need to stick and spread to obtain the best possible print [2]. Other processes where droplet impact is a crucial element are deicing [3], food conservation [4], spray painting [5], spray cooling [6], waterproofing textiles [7], and forensic research [8]; even for virus transmission in aerosols, the details of droplet impact are important [9]. Despite these wide-ranging applications, a full understanding of the droplet spreading and retraction dynamics of complex fluids is missing. This is especially true when surfactants are added to the aqueous solutions to improve spreading and coverage of the droplets, complicating the fluid dynamics. Surfactants are surface active agents that are widely employed to influence the interaction between a droplet and a surface; by lowering the surface tension of a liquid, an impacting droplet can spread more easily on a surface and exhibits a decreased retraction rate. This increases the chances of the droplet “sticking” to a hydrophobic surface instead of bouncing off. Inspired by the challenge of minimizing soil pollution due to pesticide spraying, we propose an approach to studying the impact dynamics of aqueous surfactant solutions on hydrophobic surfaces using insights into the impact process at millisecond timescales to draw conclusions about macroscopic parameters of importance to spraying applications.

Figure 1(a) shows how a water droplet bounces off a hydrophobic surface, here a cabbage leaf, which is a generic observation in pesticide spraying. On the one hand, plant surfaces are notoriously hydrophobic; on the other hand, there has been a trend towards spraying with larger droplets to

---

\*d.bonn@uva.nl

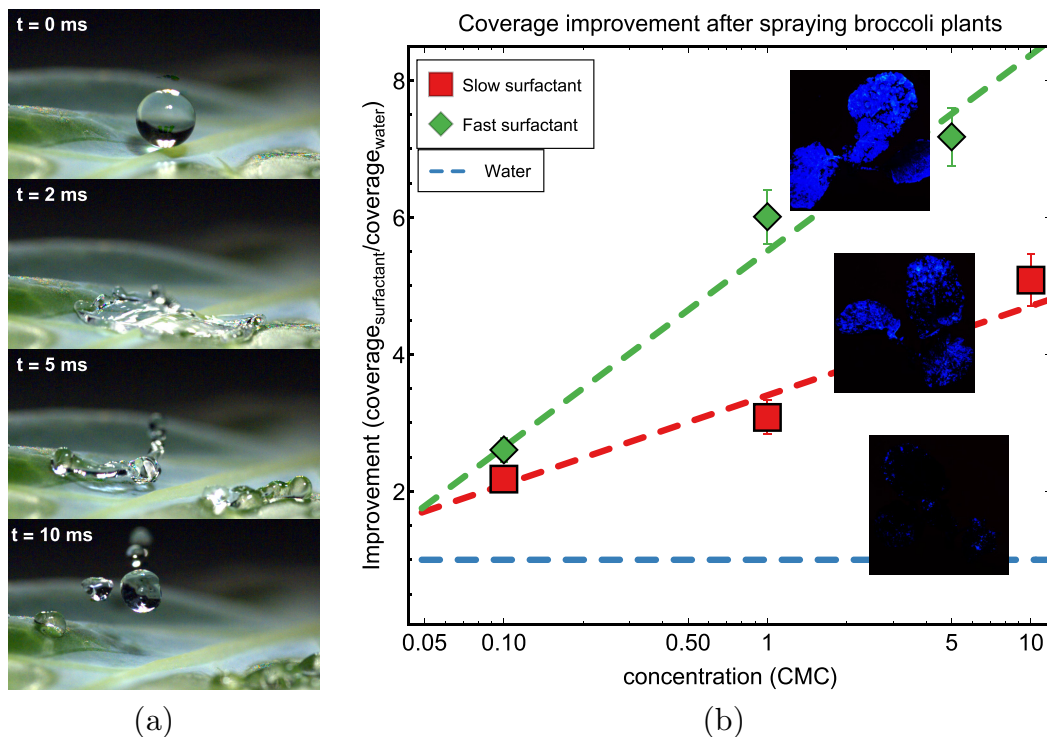


FIG. 1. Droplet rebound and coverage on plant leaves. (a) Snapshots of a water droplet bouncing off a hydrophobic cabbage leaf. (b) Relative improvement of the liquid coverage of broccoli leaves as a function of surfactant concentration. Coverage is determined from an added fluorescent, which lights up, thus indicating where the leaves are covered. The deposition improves with higher concentrations of surfactant. Even though the equilibrium surface tension of the “slow” surfactant (22 mN/m, red squares) is lower, the “fast” surfactant (32 mN/m, green diamonds) gives a better coverage.

avoid spray drift [10]. Larger droplet sizes lead to an increased chance of bounce-off, resulting in a relatively low coverage of the leaves with active ingredients and an increase of leakage into the soil. The improvement in coverage after adding different types of surfactants to a water spray, in an experiment resembling pesticide spraying, is shown in Fig. 1(b). The results show that there is a very significant difference in coverage after spraying between surfactants: surprisingly, the surfactant with the lower equilibrium surface tension results in a poorer coverage of a hydrophobic surface after spraying. It thus follows that the equilibrium surface tension is insufficient to predict the droplet behavior.

The important property governing the physics of impact, retraction, and rebound of surfactant solutions is the *dynamic* surface tension (DST). The impact and expansion of the impacting drop creates a large amount of fresh surface in a very short time, and this new surface is not necessarily covered with surfactants. The surface tension shortly after creating the new surface is higher than the equilibrium surface tension with surfactants. The surface tension can be close to the surface tension of pure water just after impact, and then decreases in time, with a characteristic timescale of the diffusion of the surfactant molecules from the bulk to the surface.

An empirical formula by Hua and Rosen [11] is often used to describe the dynamic surface tension of the droplet after creating new surface. This formula has been shown to fit well the experimental data from the bubble pressure tensiometer (BPT) [12,13]. However, Zhang and Basaran [14] show that there are competing processes caused by the DST during the spreading

TABLE I. Surfactants and their properties.

| Surfactant            | $\sigma_{eq}$ (mN/m) | CMC (g/L) |
|-----------------------|----------------------|-----------|
| Alcohol terpenes [17] | 32                   | 10        |
| AOT [17,19]           | 32                   | 1         |
| CTAB [19]             | 37                   | 0.36      |
| Glucamide             | 26                   | 1         |
| Polysorbate 20 [19]   | 34                   | 0.06      |
| Trisiloxane           | 22                   | 0.1       |

of droplets with surfactants: On the one hand the surfactant lowers the surface tension, leading to more spreading when the surfactant is faster. On the other hand stresses due to an uneven distribution of the surfactant molecules on the surface decrease spreading by Marangoni effects. Crooks, Cooper-White, and Boger [15] show that the recoil behavior of droplets containing low concentrations of surfactant does not correlate with the dynamic surface tension from the BPT, due to the Marangoni stresses caused by a heterogeneous surfactant concentration at the surface.

For simple fluids without surfactant Bartolo, Josserand, and Bonn [16] show that the retraction rate and recoil behavior of an impacting droplet is independent of impact velocity, but does depend on the surface tension of the droplet. When surfactants are present, Aytouna *et al.* [17] found that the expansion and retraction dynamics of droplets does depend on the dynamic surface tension; they make a distinction between *fast* and *slow* surfactants. Their data suggest that the characteristic time  $\tau$  with which the surfactant molecules diffuse from the bulk towards the surface determines whether a surfactant is fast ( $\tau \approx 1$  ms) or slow ( $\tau \approx 20$  ms) compared with the dynamics of the drop itself. This characteristic time decreases with increasing concentration and diffusion coefficient of the surfactant, the latter being a molecular property given roughly by the size of the surfactant molecules.

All this suggests that it is the *dynamic* surface tension that determines the interaction of the drop with the surface on short timescales. However, the typical timescale for droplet spreading is in the range of 2–3 ms [12], and current techniques for measuring the dynamic surface tension are unable to measure at this short timescale. The problem we address here is how to obtain the dynamic surface tension on such short timescales. We show below that one can infer the dynamic surface tensions of surfactant solutions in the first milliseconds after impact from the spreading dynamics of droplets themselves. This can subsequently be connected to the retraction rate which is an important indicator of droplet rebound [16].

## II. MATERIALS AND METHODS

### A. Surfactant solutions

In this paper we focus on two surfactant types: trisiloxane and alcohol terpenes, designated as slow and fast surfactant, respectively, as defined by Aytouna *et al.* [17]. Solutions were prepared in concentrations of 0.1, 0.5, 1, 5, and 10 times the critical micelle concentration (CMC) for both surfactants. For the fast surfactant, additional concentrations of 0.01 and 0.05 times the CMC were prepared. The trisiloxane and alcohol terpenes are used as a basis for this article, but also AOT, CTAB, glucamide, and polysorbate have been measured to verify the generality of our conclusions. The equilibrium surface tensions and CMC values of all surfactants are summarized in Table I. All surfactants have a density  $\rho$  of 0.997 kg/L and dynamic viscosity  $\mu$  of 1 mPa s, equal to the values of water.

### B. Droplet impact measurements

To investigate the influence of the dynamic surface tension on droplet impact, droplets were released from a syringe through a needle with a diameter of 0.5 mm. The resulting droplet diameters

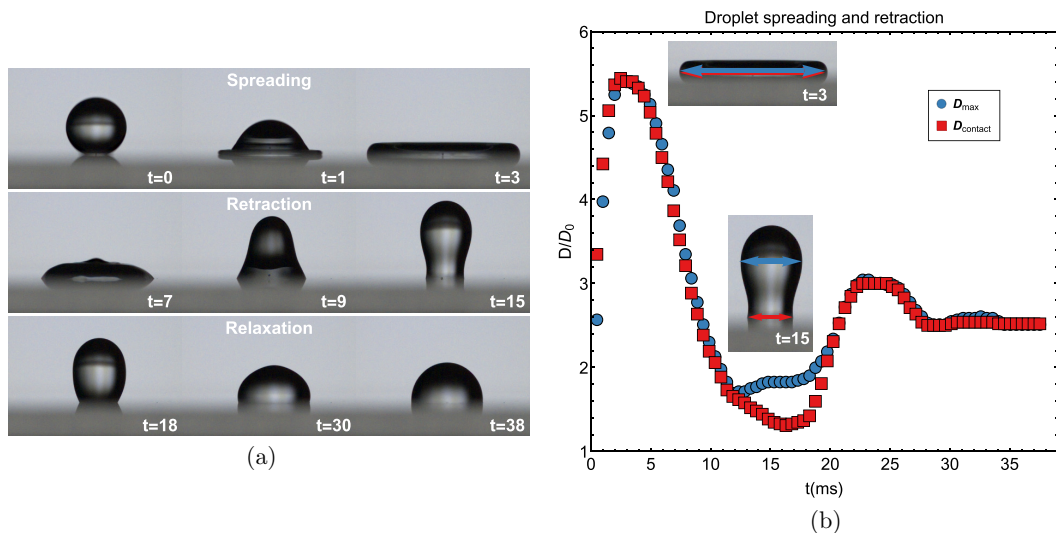


FIG. 2. (a) Image sequence of a water droplet impact showing the spreading (first row), retraction (second row), and relaxation (third row) of the droplet. Time stamps are in ms. (b) Normalized droplet diameter  $D/D_0$  as determined using the maximum diameter (red squares) and the contact line diameter (blue circles) as a function of spreading time. The impact velocity of the droplet is 1.4 m/s.

varied between 1.8 and 2.2 mm. The impact velocity  $v$  of the droplets was varied between 1.2 and 2.1 m/s by adjusting the height of the syringe. The impact of the surfactant droplets has been studied using hydrophobic silanized glass slides (contact angle  $\approx 100^\circ$ , the silanization procedure can be found in the Supplemental Material [18]) and was recorded with a high-speed camera (Phantom Miro M310) with a frame rate of 8100 frames per second and a spatial resolution of  $\approx 50$  pixels per mm. All uncertainties were obtained by calculating the standard deviation between at least five repetitions. Wherever the error bar is not shown, it is smaller than point size.

The diameter  $D(t)$  of the droplet was determined by measuring the maximum diameter of the droplet in each image of the image sequence. A typical example of such an image sequence is shown in Fig. 2(a). Using the maximum diameter is different from other studies, who use the diameter at the contact line [16]. In Fig. 2(b) we compare the diameters obtained by using both methods for a typical water droplet impact at  $v = 1.4$  m/s. We find that the maximum diameter (blue circles) and contact line diameter (red squares) are identical during spreading (0–3 ms) and retraction (3–10 ms). There is a deviation between the two diameters between 10 and 20 ms after impact, as the droplet almost detaches from the surface due to a high retraction rates [see inset of Fig. 2(b)]. However, this deviation has no influence on the analysis of droplet spreading, as the maximum spreading diameter and contact line diameter are identical at maximum spreading [ $t = 3$  ms; see inset Fig. 2(b)], which is the diameter used to determine the dynamic surface tension. The two diameters overlap until right before the minimum, so that the retraction rates obtained from both diameter profiles are also identical.

### C. How to obtain the dynamic surface tension

Our millisecond timescale measurements of the droplet spreading and subsequent retraction allow us to gain insight into the dynamic surface tension at the relevant timescale. This is done along two lines of analysis.

First, we use the maximum spreading diameter  $D_{\max}$  of the drop compared with the original diameter  $D_0$ . This parameter follows from a balance between the inertial forces that drive droplet

expansion, and the viscous and capillary forces that resist it. The resulting maximum spreading ratio  $D_{\max}/D_0$  is then given by [8]

$$\frac{D_{\max}}{D_0} = \text{Re}^{1/5} \frac{\sqrt{\text{We Re}^{-2/5}}}{1.24 + \sqrt{\text{We Re}^{-2/5}}}, \quad (1)$$

where  $\text{We} = \rho v^2 D_0 / \sigma_{\text{eff}}$  is the Weber number and  $\text{Re} = \rho v D_0 / \mu$  is the Reynolds number, both functions of density  $\rho$ , impact velocity  $v$ , initial diameter  $D_0$ , effective surface tension  $\sigma_{\text{eff}}$  and dynamic viscosity  $\mu$ . For a surfactant solution, the capillary force resisting the expansion will be given by the instantaneous value of the dynamic surface tension. The effects of this time-dependent surface tension are reflected in an effective surface tension  $\sigma_{\text{eff}}$ . To first order, we approximate the effective surface tension over the spreading process [ $t$  ranging from 0 (moment of impact) to  $t_{\max}$  (moment of maximum spreading)] by the surface tension at  $t_{\max}$ , so  $\sigma_{\text{eff}} \approx \sigma(t = t_{\max})$ .

A second method to determine the dynamic surface tension at maximum spreading is by using the timescale of the spreading. The time from the start of the impact to the maximal spreading  $t_{\max}$  was analyzed by Bartolo, Josserand, and Bonn [16], who found the following equation for the inertial timescale  $t_i$  of a droplet impact in the inertial regime [20]:

$$t_i = C \sqrt{\frac{\rho R_i^3}{\sigma}}, \quad (2)$$

where  $C$  is a proportionality constant,  $\rho$  is the density of the fluid,  $R_i$  is the droplet radius, and  $\sigma$  is the surface tension of the fluid, here again taken at the moment of maximum spreading. Note that this time of spreading is predicted to be independent of the impact velocity. Although the viscous forces are small in the experiments presented here, they do affect the dynamics and therefore the proportionality constant  $C$  in Eq. (2). Therefore, we establish the proportionality constant experimentally using water, as all the surfactant solutions used here have the same viscosity as water. This is shown in Sec. II D.

To connect our measurements of the dynamic surface tension to the equilibrium value, we use the empirical formula by Hua and Rosen [11]

$$\sigma(t) = \sigma_{\infty} + \frac{\sigma_0 - \sigma_{\infty}}{1 + \left(\frac{t}{\tau}\right)^n}, \quad (3)$$

where  $\sigma_{\infty}$  is the equilibrium surface tension of the surfactant,  $\sigma_0$  is the surface tension of water (72 mN/m),  $\tau$  is a characteristic time for the surfactant molecules to reach the droplet surface, and  $n$  is a fit parameter that we fix here at a value of 1 [21]. Using a bubble pressure tensiometer (BPT) to measure the surface tension over a time range of 15–16 000 ms, we can use the above equation to extrapolate  $\sigma$  to  $t = t_{\max}$  (on the order of a few ms).

#### D. Calibration with water

To obtain the dynamic surface tension from the time of spreading ( $t_i$ ), the proportionality constant in Eq. (2) was determined from the spreading of water droplets, where the surface tension is constant at 72 mN/m. A proportionality constant of 0.67 was obtained. Note that for impact velocities below 1 m/s, the  $t_i$  method does not work, as the surface tension that obtained from the  $t_i$  method for water is found to be much lower than the expected value. This could be explained by the fact that the droplet inertia does not dominate the viscous effects during droplet retraction at these low impact velocities. Although the droplet spreading ratio  $D_{\max}/D_0$  is dependent on the surface wettability at low impact velocities [22–24], the surface wettability does not seem to affect droplet spreading enough to significantly influence the calculation of the surface tension from this method at the measured impact velocities. This is likely due to the fact that the influence of surface wettability is minimal for hydrophobic surfaces [24]. These results show that both the spreading ratio and  $t_i$  methods could be used to measure the surface tension of the liquid during droplet impact.

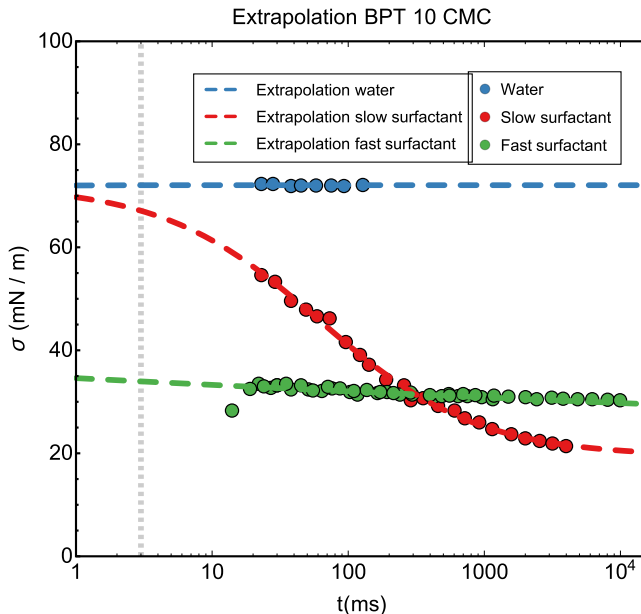


FIG. 3. Surface tension as determined from bubble pressure tensiometer measurements as a function of surface age (time that has passed since the creation of the surface) for 10 CMC concentrations of the fast (green diamonds) and slow (red squares) surfactants and water (blue circles, constant at 72 mN/m). The dashed lines are the best fits of Eq. (3) to the experimental data. These fits are used to extrapolate the dynamic surface tension of the liquids to the typical time of spreading of a droplet, which is 3 ms (gray dotted line). Fit parameters  $\sigma_0$  (mN/m),  $\sigma_\infty$  (mN/m),  $\tau$  (s),  $n$  are  $\sigma_0 = 72$ ,  $\sigma_\infty = 19.4$ ,  $\tau = 62.1$ ,  $n = 7.51 \times 10^{-1}$  (slow),  $\sigma_0 = 72$ ,  $\sigma_\infty = 18.3$ ,  $\tau = 9.83 \times 10^{-8}$ ,  $n = 5.13 \times 10^{-2}$  (fast).

### III. RESULTS AND DISCUSSION

#### A. Bubble pressure measurement

For comparison, the dynamic surface tension was measured with a Krüss Bubble Pressure Tensiometer BP50. This apparatus allowed us to measure the dynamic surface tension of the solutions for a minimum surface age of 15 ms and measuring up to a surface age of 16 000 ms. Figure 3 shows the measured time dependencies of the dynamic surface tension with the bubble pressure tensiometer for water and the fast and slow surfactants. The concentration of both surfactants is 10 CMC. The results for the other concentrations can be found in the Supplemental Material [18]. These measurements show that the surface tension of the fast surfactant (green diamonds) are well below the slow surfactant (red squares), despite the equilibrium surface tension being higher. These results are calibrated to the constant surface tension of water of 72 mN/m (blue circles). As the typical time of spreading of a droplet ( $\approx 3$  ms) is outside the measurement range of the bubble pressure tensiometer, we extrapolate to this timescale by fitting Eq. (3) to the experimental data (dotted lines in Fig. 3).

#### B. Droplet spreading and retraction

Figure 4 shows how droplets of water, a fast-surfactant (mix of alcohol terpenes) and a slow-surfactant (trisiloxane) solution typically behave during impact on a hydrophobic (silanized) glass slide. The droplet sizes are similar to what is used in pesticide spraying nowadays, and also similar to the situation of Fig. 1(b) where we sprayed broccoli leaves. The surface is a model hydrophobic surface with a contact angle of  $\approx 100^\circ$ . We observe that the droplet containing the slow surfactant



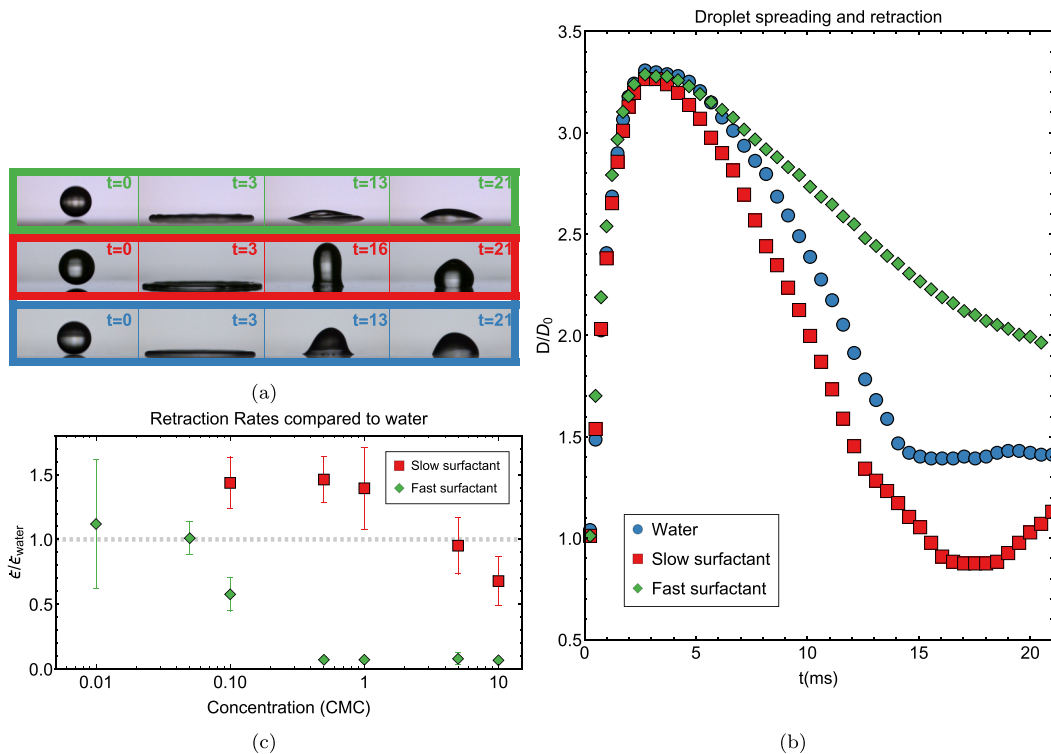


FIG. 4. Droplet spreading and retraction. (a) Snapshots of typical droplet spreading for water (in blue), slow surfactant solution (0.1 CMC; in red) and fast surfactant (0.1 CMC; in green) impacting at a speed of 1.9 m/s. Time stamps are in ms. Maximum spreading is reached at 3 ms, equilibrium around 21 ms. Conventional surface tension measurement techniques do not reach these timescales. (b) Normalized droplet diameter  $D/D_0$  as a function of time for the same droplets as shown in panel (a). (c) Retraction rate  $\dot{\epsilon}$  normalized by the retraction rate of water ( $\dot{\epsilon}_{\text{water}} = 50 \text{ s}^{-1}$  at an impact speed of 1.9 m/s), as a function of surfactant concentration.

retracts faster than water, especially when the impact speed is high. As a result, this droplet is more prone to bounce-off. This is also visible in the snapshots of the droplet impact [Fig. 4(a)] and in the evolution of the droplet diameter as function of time [Fig. 4(c)]. The retraction rate of the fast surfactant, on the other hand, is lower than that of water, and the droplet retracts less: this surfactant does a good job in improving deposition, as indeed observed in Fig. 1(b). These findings agree with those of Zhang and Basaran [14], who showed that the retraction of a droplet containing a slow surfactant can be faster than for water and attributed this to Marangoni stresses caused by uneven distribution of the surfactant molecules along the surface.

### C. Results for the dynamic surface tension

The surface tension at maximum spreading as calculated using both the maximum diameter [Eq. (1)] and time of spreading [Eq. (2)] are shown in Fig. 5 for an impact speed of 1.6 m/s and different surfactant concentrations. It can be seen that both methodologies yield the same results and that they are in good agreement with the results from the bubble pressure extrapolation for this impact velocity. However, other impact velocities yield effective dynamic surface tensions that are slightly below (low  $v$ ) or above (high  $v$ ) the bubble pressure extrapolation (see Fig. 6 and Supplemental Material [18]). This tells us that the bubble pressure measurement does not give us



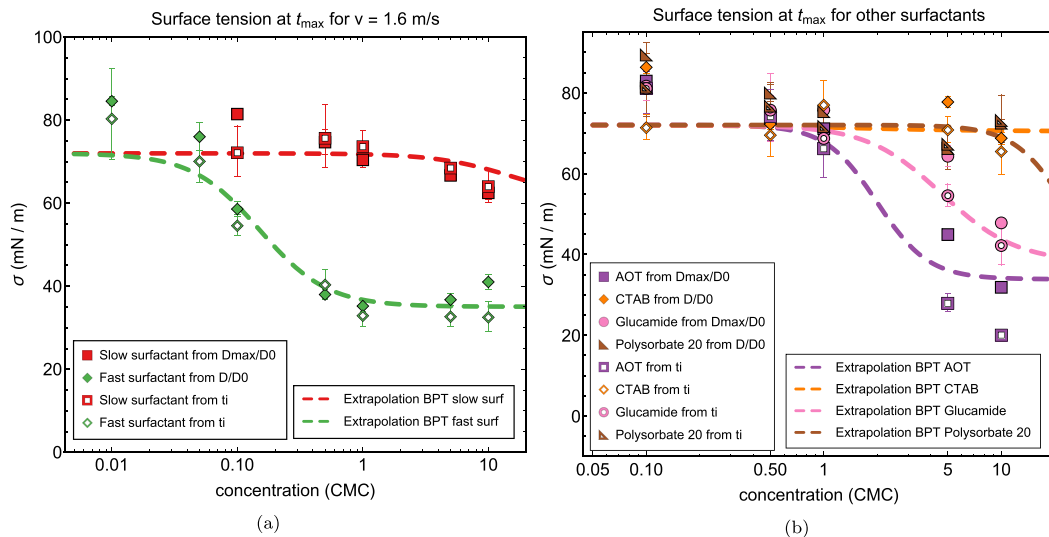


FIG. 5. Effective dynamic surface tension at maximum spreading. Dynamic surface tension  $\sigma$  calculated using the two methods described in the main text as a function of fast (green diamonds) and slow (red squares) surfactant concentration for (a) medium impact velocity  $v = 1.6$  m/s. The dotted lines are extrapolations based on BPT measurements (see Supplemental Material [18]) and Eq. (3). (d) Dynamic surface tension at maximum spreading as a function of surfactant concentration for other surfactants (AOT, CTAB, glucamide, and polysorbate 20) as calculated using the two methods described in the text. Impact velocity  $v = 1.6$  m/s. The dotted lines are extrapolations based on BPT measurements and Eq. (3).

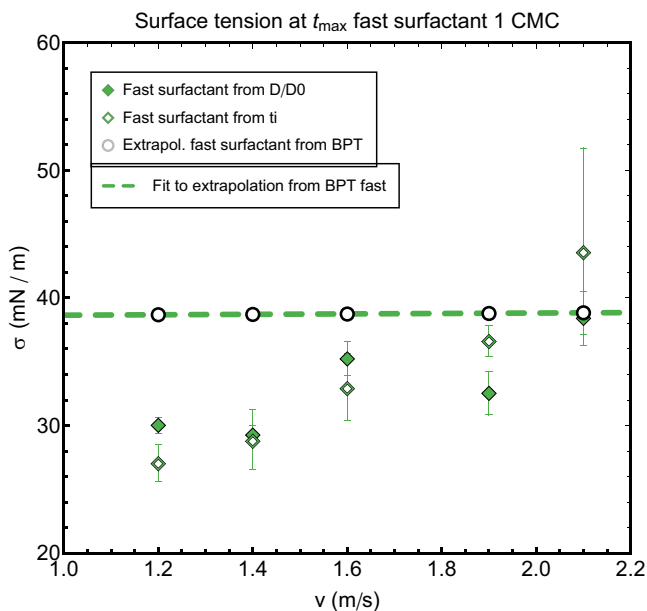


FIG. 6. Dynamic surface tension at maximum spreading as a function of droplet impact velocities for a solution of fast surfactant with a concentration of 1 CMC. The dotted line is the extrapolation of BPT measurements using Eq. (3).

the full information about the surface tension at droplet impact, since it cannot take into account impact velocity, which our new methods of obtaining the DST *can* do.

Figure 5 shows that the effective dynamic surface tension of the slow surfactant reaches values even *higher* than the surface tension of water (72 mN/m). That the effective surface tension values for the surfactant solutions can be higher than that of water is likely due to Marangoni stresses [14], resulting from an uneven distribution of surfactant molecules along the surface.

Similar results of the effective dynamic surface tension are observed for a range of other surfactants; dioctyl sulfosuccinate sodium salt (AOT), cetrimonium bromide (CTAB), glucamide, and polysorbate 20 as can be seen in Fig. 5(b). Similar to Fig. 5, the obtained surface tensions of the higher concentrations are lower than those of the lower concentrations and the extrapolation of the bubble pressure tensiometer gives similar surface tensions at medium impact speed of 1.6 m/s. A difference between fast (AOT, glucamide) and slow (CTAB, polysorbate 20) surfactants can be observed.

The influence of the impact velocity on the dynamic surface tension of the droplets at maximum spreading can be observed in Fig. 6: the surface tension, determined with the droplet spreading ratio (solid symbols) and  $t_i$  (open symbols), increase with increasing impact velocity. The results are compared with an extrapolation of the BPT measurements (dotted line and white circles), which is independent of impact velocity. The difference in time of spreading between the different impact velocities [the time that we use to calculate the dynamic surface tension using Eq. (3)] is so small that it does not translate into a significant variation in surface tension from the BPT. From the impact dynamics is to see that the effective surface tension depends on the impact velocity. The difference can be explained from the fact that the dynamic surface tension at maximum spreading results from a competition between the rate of formation of new droplet surface and the rate at which the surfactants arrive at the interface from the liquid bulk. So formally  $D_{\max}$  follows from  $\sigma(t)$  with  $t$  between 0 and  $t_{\max}$  and not from  $\sigma(t_{\max})$ ; however it turns out that the latter is a good and easily implementable approximation. Higher droplet impact velocities imply faster droplet spreading, and hence a higher rate of surface area formation, leading to a smaller decrease in surface tension for the same concentration of surfactant. It therefore follows that our method is more accurate than the BPT.

#### D. Retraction rate

We now extend our analysis to  $t > t_{\max}$ , which is when the droplet retracts. The retraction phenomenon is particularly relevant to spraying applications, as it was found that above a critical retraction speed, bounce-off occurs, with the droplet (partially) disconnecting from the surface after impact [1]. Therefore, the retraction rate is an indicator of bounce-off, and hence of poor coverage during spraying. How a droplet retracts after impact is strongly influenced by the surface tension. The retraction rate has been previously defined as

$$\dot{\epsilon} = V_{\text{ret}}/R_{\max} \propto t_i^{-1} = \sqrt{\frac{\sigma}{\rho R_i^3}}, \quad (4)$$

where  $V_{\text{ret}}$  is the maximum slope during retraction,  $R_{\max}$  is the maximum radius of the droplet during spreading and  $\sigma$ ,  $\rho$ , and  $R_i$  are the surface tension, density, and initial diameter of the droplet, respectively [16].

Figure 7(a) shows the retraction rate  $\dot{\epsilon}$  of the droplets containing fast and slow surfactant as function of the dynamic surface tension at the moment the droplet has spread to its maximum diameter  $D_{\max}$ . Note that the retraction rate above which bounce-off is expected to occur,  $\approx 100$  mm/s, is not reached in these experiments. We find that above a critical value of  $\sigma(t_{\max})$ , the droplet retraction rates roughly follow the predicted  $\sqrt{\sigma}$  dependence. The retraction rate can be made dimensionless by looking at  $\dot{\epsilon} t_i$  versus the inverse Ohnesorge number ( $\text{Oh} = \mu/\sqrt{\rho\sigma R_i}$ ). This is shown in Fig. 7(b). A linear fit through the data is shown, which is the predicted behavior of the dimensionless retraction rate in the capillary regime by Bartolo, Josserand, and Bonn [16]. The

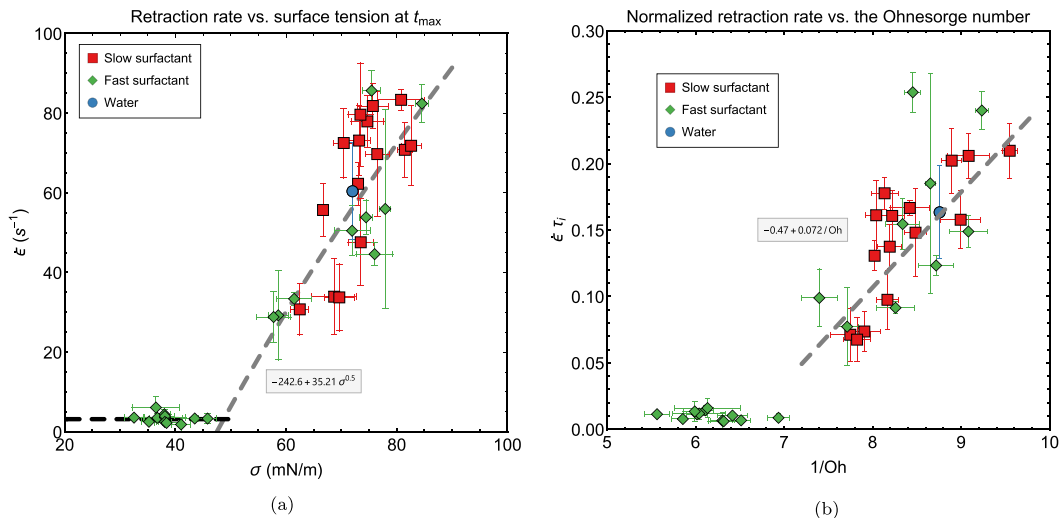


FIG. 7. (a) Retraction rate  $\dot{\epsilon}$  of droplets for  $1.7 < v < 2.1$  m/s plotted against surface tension calculated from  $D_{\max}/D_0$ . The dotted line is the prediction by Eq. (4). (b) Dimensionless retraction rate versus  $1/Oh$ . The dotted line is the best fit to the data  $\propto 1/Oh$ .

uncertainties of the data are still quite large and additional research over a larger range would be necessary to quantitatively confirm this exact relation. However, the most important message to take from Fig. 7 is that higher dynamic surface tensions lead to higher retraction rates. At high concentrations of the fast surfactant and hence low surface tensions, the droplet retraction rate reaches a minimum.

Because the retraction rate is a leading parameter that determines droplet bounce-off, the observed dynamic surface tensions explain why the coverage of hydrophobic surfaces with fast surfactants is higher than with slow surfactants. In line with our observations, Aytouna *et al.* [17] reported bounce-off on hydrophobic parafilms for a slow surfactant and no bounce-off for a fast surfactant with the same  $\sigma_{eq}$ .

Our analysis can be used to further refine our understanding of droplet impact on realistic surfaces, and to find the optimum surfactant properties and concentrations to influence this process. Progress in preventing droplet rebound could for example reduce the use of expensive or contaminating chemicals and their leakage into the environment or increase precision in applications like high-performance inkjet printing. In other processes, like forensic research, a refined understanding of this process can be used to get a better insight in situations where droplet impact is crucial for reconstructions.

#### IV. CONCLUSIONS

We used two methods to obtain the dynamic surface tension of impacting droplets at the impact timescale. In this article we focus on two different surfactant types: one fast surfactant and one slow surfactant. Our measurements quantitatively reveal for the first stage of the droplet impact process that the dynamic surface tension of a solution with a fast surfactant is lower than that of a solution containing a slow surfactant, which we attribute to the inability of slow surfactant molecules to diffuse to the droplet surface at these short timescales. Measurements for a range of other surfactants yield very similar results.

When we vary the droplet impact velocity we find small variations in the dynamic surface tension evaluated at  $D_{\max}$ . This can be explained by the fact that higher droplet impact velocities result in

faster droplet spreading, and hence a higher rate of surface area formation, leading to a smaller decrease in surface tension for the same concentration of surfactant.

We find a relation between the dynamic surface tension and the retraction rate of the impacting droplets that is in agreement with the literature [16]. Because the retraction rate is a leading parameter that determines droplet bounce-off, the observed dynamic surface tensions explain why the coverage of hydrophobic surfaces with fast surfactants is higher than with slow surfactants.

In conclusion, our measurements provide experimental verification of previous predictions, such as of the relation between long timescale surface tension and dynamic surface tension at the moment of maximum droplet spreading, and of the relation between droplet retraction rate and dynamic surface tension.

#### ACKNOWLEDGMENTS

This work is part of an Industrial Doctorate contract between the University of Amsterdam and the company Green A B.V. that is supported by the Netherlands Organization for Scientific Research (NWO) under project number NWA.ID.17.016. The authors would like to thank P. Kolpakov for the silanization of the glass slides.

H.H. and R.S. contributed equally to this paper.

- 
- [1] V. Bergeron, D. Bonn, J. Y. Martin, and L. Vovelle, Controlling droplet deposition with polymer additives, *Nature (London)* **405**, 772 (2000).
  - [2] B. Zhmud and F. Tiberg, Surfactants in ink-jet inks, *Surfactants Polym. Coat. Inks Adhes.* **1**, 211 (2003).
  - [3] Y. H. Yeong, R. Mudafort, A. Steele, I. Bayer, E. Loth, and G. De Combarieu, Water droplet impact dynamics at icing conditions with and without superhydrophobicity, in *4th AIAA Atmospheric and Space Environments Conference* (American Institute of Aeronautics and Astronautics, Reston, VA, USA, 2012), p. 3134.
  - [4] R. Andrade, O. Skurtys, and F. Osorio, Drop impact behavior on food using spray coating: Fundamentals and applications, *Food Res. Int.* **54**, 397 (2013).
  - [5] G. N. Carlton, A model to estimate a worker's exposure to spray paint mists, Technical Report No. ADA311669, University of North Carolina (1996).
  - [6] J. Kim, Spray cooling heat transfer: The state of the art, *Int. J. Heat Fluid Flow* **28**, 753 (2007); Including Special Issue of Conference on Modelling Fluid Flow (CMFF'06), Budapest.
  - [7] D. S. Vernez, P.-O. Droz, C. Lazor-Blanchet, and S. Jaques, Characterizing emission and breathing-zone concentrations following exposure cases to fluororesin-based waterproofing spray mists, *J. Occup. Environ. Hyg.* **1**, 582 (2004).
  - [8] N. Laan, K. G. De Bruin, D. Bartolo, C. Josserand, and D. Bonn, Maximum Diameter of Impacting Liquid Droplets, *Phys. Rev. Applied* **2**, 044018 (2014).
  - [9] G. A. Somsen, C. van Rijn, S. Kooij, R. A. Bem, and D. Bonn, Small droplet aerosols in poorly ventilated spaces and SARS-CoV-2 transmission, *Lancet Respir. Med.* **8**, 658 (2020).
  - [10] S. L. Bird, D. M. Esterly, and S. G. Perry, Off-target deposition of pesticides from agricultural aerial spray applications, *J. Environ. Quality* **25**, 1095 (1996).
  - [11] X. Y. Hua and M. J. Rosen, Dynamic surface tension of aqueous surfactant solutions: I. Basic parameters, *J. Colloid Interface Sci.* **124**, 652 (1988).
  - [12] N. Mourougou-Candoni, B. Prunet-Foch, F. Legay, M. Vignes-Adler, and K. Wong, Influence of dynamic surface tension on the spreading of surfactant solution droplets impacting onto a low-surface-energy solid substrate, *J. Colloid Interface Sci.* **192**, 129 (1997).
  - [13] J. Eastoe and J. S. Dalton, Dynamic surface tension and adsorption mechanisms of surfactants at the air-water interface, *Adv. Colloid Interface Sci.* **85**, 103 (2000).
  - [14] X. Zhang and O. A. Basaran, Dynamic surface tension effects in impact of a drop with a solid surface, *J. Colloid Interface Sci.* **187**, 166 (1997).

- [15] R. Crooks, J. Cooper-White, and D. V. Boger, The role of dynamic surface tension and elasticity on the dynamics of drop impact, *Chem. Eng. Sci.* **56**, 5575 (2001).
- [16] D. Bartolo, C. Josserand, and D. Bonn, Retraction dynamics of aqueous drops upon impact on non-wetting surfaces, *J. Fluid Mech.* **545**, 329 (2005).
- [17] M. Aytouna, D. Bartolo, G. Wegdam, D. Bonn, and S. Rafai, Impact dynamics of surfactant laden drops: Dynamic surface tension effects, *Exp. Fluids* **48**, 49 (2010).
- [18] See Supplemental Material at <http://link.aps.org/supplemental/10.1103/PhysRevFluids.6.033601> for surface preparation and results for other surfactants.
- [19] R. Sijts, S. Kooij, and D. Bonn, How surfactants influence the drop size in sprays, [arXiv:1907.09723](https://arxiv.org/abs/1907.09723).
- [20] D. Richart, C. Clanet, and D. Quéré, Contact time of a bouncing drop, *Nature (London)* **417**, 811 (2002).
- [21] R. Sijts and D. Bonn, The effect of adjuvants on spray droplet size from hydraulic nozzles, *Pest Manage. Sci.* **76**, 3487 (2020).
- [22] J. B. Lee, N. Laan, K. G. de Bruin, G. Skantzaris, N. Shahidzadeh, D. Derome, J. Carmeliet, and D. Bonn, Universal rescaling of drop impact on smooth and rough surfaces, *J. Fluid Mech.* **786**, R4 (2015).
- [23] S. Wildeman, C. W. Visser, C. Sun, and D. Lohse, On the spreading of impacting drops, *J. Fluid Mech.* **805**, 636 (2016).
- [24] T. C. de Goede, K. G. de Bruin, N. Shahidzadeh, and D. Bonn, Predicting the maximum spreading of a liquid drop impacting on a solid surface: Effect of surface tension and entrapped air layer, *Phys. Rev. Fluids* **4**, 053602 (2019).